International Journal of Chemical, Materials and Biomolecular Sciences
ISSN: 2415-6620
Vol:8, No:11, 2014

Deformability of the Rare Earth Metal Modified Metastable-β Alloy Ti-15Mo

F. Brunke, L. Waalkes, C. Siemers

***Abstract*—**Due to reduced stiffness, research on second generation titanium alloys for implant applications, like the metastable β-titanium alloy Ti-15Mo, become more and more important in the recent years. The machinability of these alloys is generally poor leading to problems during implant production and comparably large production costs. Therefore, in the present study, Ti-15Mo was alloyed with 0.8 wt.-% of the rare earth metals lanthanum (Ti-15Mo+0.8La) and neodymium (Ti-15Mo+0.8Nd) to improve its machinability. Their microstructure consisted of a titanium matrix and micrometer-size particles of the rare earth metals and two of their oxides. The particles stabilized the microstructure as grain growth was minimized. As especially the ductility might be affected by the precipitates, the behavior of Ti-15Mo+0.8La and Ti-15Mo+0.8Nd was investigated during static and dynamic deformation at elevated temperature to develop a processing route. The resulting mechanical properties (static strength and ductility) were similar in all investigated alloys.

***Keywords*—**Ti-15Mo, Titanium alloys, Rare earth metals, Free-machining alloy.

I. Introduction

THE requirements for materials in medical applications are immense. Implant alloys have to exhibit high specific static and dynamic strengths, a low Young's modulus, good corrosion resistance, and biocompatibility. Titanium and its alloys fulfill all these requirements best beyond all possible metallic alloys. Therefore, first generation α- or (α+β)-Titanium alloys like CP-Titanium Grade 2 and Grade 4, Ti-6Al-4V and Ti-6Al-7Nb are used in surgical applications for more than two decades now [1], [2].

Besides all the benefiting properties of the first generation alloys, the application of these first generation implant alloys is problematic: First, in the recent years, the interaction of aluminum and vanadium with the human body was intensively discussed and investigated. Both elements were suspected to lead to long term health problems. It is known that higher concentrations of aluminum might cause the Alzheimer's disease and vanadium as well as vanadium oxides are cytotoxic. Second, the stiffness can be up to five times higher than that of human long bones. Thus, stress shielding is observed leading to degradation of the bone and loosening of the implant. [2], [3].

Consequently, research is focused on titanium alloys with non-critical alloying elements like niobium, molybdenum, iron and silicon leading to the introduction of new alloys in the 1990ies. These second generation implant alloys like Ti-15Mo belong to the class of the solute-lean metastable-β alloys. These alloys can be solution treated ($R_m \approx 650$ N/mm²) and water quenched to gain a β-matrix which can be afterwards aged to achieve higher strength by the precipitation of fine α-phase ($R_m \approx 1200$ N/mm²). In addition, additional metastable phases like α" or ω might occur leading to extra strengthening. In the solution treated state the stiffness is about 25% lower compared to Ti-6Al-4V and Ti-6Al-7Nb which only slightly increases during ageing [4], [5].

Casting and welding of titanium alloys are critical processes in implants exposed to dynamic bending, as the unavoidable porosity and microstructure changes might reduce the fatigue life. Therefore, hip or knee implants are typically produced by forging followed by different machining operations. Depending of the final contour, the material removal can be up to 50% of the semi-finished product [6]. Due to their mechanical, physical and chemical properties titanium alloys can only be machined with low cutting speeds and feed rates. In addition, long chips are formed during machining operations, especially in turning and drilling. These long chips can wrap around the workpiece, the turning chisel or get stuck between the drill and the hole which is leading to poor surface quality, rapid tool wear or complete tool failure. Hence, the operator has to interrupt the machining process as often as it is necessary to remove the long chips. Therefore, machining operations of titanium alloys are difficult to be automated which makes the process time-consuming and cost intensive [7].

The chip formation process of different titanium alloys has been studied in experiments and simulations in detail [8]-[10]. α-, (α+β)- and aged metastable β-titanium alloys form so-called segmented chips having a saw-tooth like structure for almost all cutting speeds, whereas solution treated metastable β-alloys show a cutting speed dependent change in the chip morphology from continuous chips (constant chip thickness) at low speeds to segmented chips at higher cutting speeds [12].

During segmented chip formation, the deformation in the primary shear zone is concentrated in a narrow region leading from the tool tip to the uncut surface. During further progress of the tool, the deformation further localizes and finally a shear band is formed which separates the segments. During the shear band formation, the temperature can locally exceed 1000°C [11], [12].

The solubility of all the rare earth metals in titanium is very low in the liquid as well as in the solid state. During crystallization, titanium (melting point approx. 1670°C)

F. Brunke, L. Waalkes, and C. Siemers are with the Institute for Materials of the Technische Universität Braunschweig, 38106 Braunschweig, Germany (phone: 0049-(0)531-391-3073; fax: 0049-(0)531-391-3058; e-mail: f.brunke@tu-braunschweig.de, l.waalkes@tu-braunschweig.de, c.siemers@tu-braunschweig.de).

solidifies first and the remaining melt is enriched in e.g. lanthanum (920°C) or neodymium (1024°C). This enriched melt is pushed forward by the solidification front and finally crystallizes on the grain boundaries where equiaxed lanthanum-rich or neodymium-rich particles are formed. During rapid solidification, some particles might also be trapped within the grains.

Metallic lanthanum or neodymium particles located in the shear zone start to soften or even melt during machining (in case of segmented chip formation). This causes a reduced adhesion between the segments, the chips can easily separate and short chip formation is observed [11]. As a result, improved surface quality is observed and machining operations can be automated. Related alloys, e. g. Ti-6Al-4V-0.9La and Ti-6Al-2V-3Nb-0.7Fe-0.3Si-0.9La have been successfully developed [12]. The disadvantage of these modified alloys is a reduced fatigue strength and ductility. Additionally, coarsening of the particles during hot deformation can lead to cracking of the material. Therefore further investigations were carried out to discover the influence of different amounts of rare earth metals in relation to alloying elements like iron, niobium or copper [13]-[15].

In the present study, the chemical composition of Ti-15Mo alloy was modified by the addition of lanthanum and neodymium to enhance the machinability. The main focus was to investigate the influence of the particles on the microstructure, the phase composition and, especially, on the deformability. Therefore, static (compression test) and dynamic (rotary swaging) deformation experiments were performed. Afterwards the deformed and annealed material was investigated with respect to its mechanical properties.

II. Experimental Details

A. Alloy Production and Heat Treatments

The Ti-15Mo alloy used in our experiments has been produced by the Gesellschaft für Elektrometallurgie GmbH (GfE) in Nuremberg, Germany.

For each experimental alloy an amount of approximately 350 g Ti-15Mo together with 0.8wt.-% lanthanum (purity 99.9%) or neodymium (99.9%) were molten in a laboratory-size plasma-beam cold-hearth melting furnace (PB-CHM). After a first melting step, the ingots were turned and twice remelted. Finally, the alloys were cast into a water-cooled cylindrical copper mold (diameter: approx. 13 mm, height: 85 mm). Ti-15Mo has been processed in the same way (remelting only) as a reference material.

After melting and casting, all bars have been solution treated (ST) at 800°C in the β phase field for 30 minutes in air and were afterwards water quenched to remove possible residual stresses from the casting process and to produce similar starting conditions for all alloys.

B. Microstructure and Particles Analyses

Discs of 0.5-1.0mm were cut of the bars after casting and the solution treatment to investigate the microstructure. All the samples were mechanically grinded to remove the oxide layer as well as the α-case formed during the ST heat treatment. Afterwards, the samples were warm embedded and the cross-sections were prepared by grinding with SiC paper starting with grain size P180 to a final grain size of P2500. Due to the affection to smearing of Ti-15Mo alloy the P600 step was repeated. Furthermore, the P2500 discs were rubbed with wax to avoid scratch formation. After grinding the samples were polished with diamond suspension (6 µm and 3 µm). For final polishing a mixture of OPS (50ml) and H_2O_2 (10ml) was used. All the samples were etched with a Kroll's reagent (3 ml HF, 6 ml HNO_3, 100 ml H_2O).

The microstructure of the samples was analyzed by means of a Zeiss Imager.M2m optical microscope and by a Leo Gemini 1550 scanning electron microscope. The grain and particle size was determined manually using more than 50 measurements for each sample.

C. Deformation

Compression tests were performed at elevated temperatures (700°C, 750°C and800°C) to investigate the deformation behavior of the alloys. Samples of diameter 11 mm and height 18 mm were compressed with a rate of 1.8 mm/s to a final height of 7 mm (degree of deformation approx. 0.9) and the resulting flow curves were recorded. To minimize friction, the samples were coated with a copper-based paste. After deformation, the samples were furnace-cooled. Microstructure investigations were in the deformed and deformed + ST state as described in the previous section.

Dynamic deformation was carried out by rotary swaging. The samples (diameter: 13 mm, height: 70 mm) were coated with a zirconia to hinder welding with the tool. The samples were heated up on 805°C for 22 minutes in an external tube furnace and deformed at approximately 775°C. Three steps (12 mm, 11 mm, 10 mm) of deformation were done (overall degree of deformation approx. 0.3).

D. Phase Analysis

Phase analyzes (as cast, ST, deformed, deformed + ST) were performed by means of hard X-rays at beamline P07 of PETRA III, HASYLAB, DESY. The samples were investigated in transmission (Debeye-Scherrer configuration) and the resulting diffraction patterns were recorded by a Perkinson-Elmer 16 inch detector [16].

The energy of the beam was chosen to 99 keV leading to a wavelength of λ= 0.01276 nm and the samples were exposed to the beam for 0.5 seconds. 15 frames were averaged to achieve the final XRD pattern for each measurement; five points (area of exposure 0.5 mm x 0.5 mm) were investigated for each sample.

The diffraction patterns were integrated (2 theta angle) using the fit2D software [17]. Afterwards the CMPR Logic software [18] was used together with a PDF 2 database (release 2005) to calculate and identify the peak positions of β-, α-, and ω-phases as well as the present lanthanum- and neodymium-phases.

E. Mechanical Properties

The static mechanical properties were determined by

automated Vickers hardness measurements (HV10) using the metallographic cross-sections. In addition, tensile tests were performed at room temperature on deformed and solution treated bars (rotary swaging + ST).

III. Results and Discussion

In the solution treated state, the microstructure of the alloys consisted of equiaxed β-grains. The lanthanum particles were dispersed mainly on the grain boundaries while the neodymium particles were segregated in the matrix too (see Figs. 1-3). The average grain size of the modified alloys was decreased by 50% compared to the standard alloy, see Table I.

Heat treatments, especially in the single phase region, lead to grain coarsening of the standard alloy, whereas the modified alloys did not show grain growth. In earlier investigations a microstructure stabilizing effect of particles for (α+β)-alloys was observed as well [19].

The average hardness was similar for all three alloys.

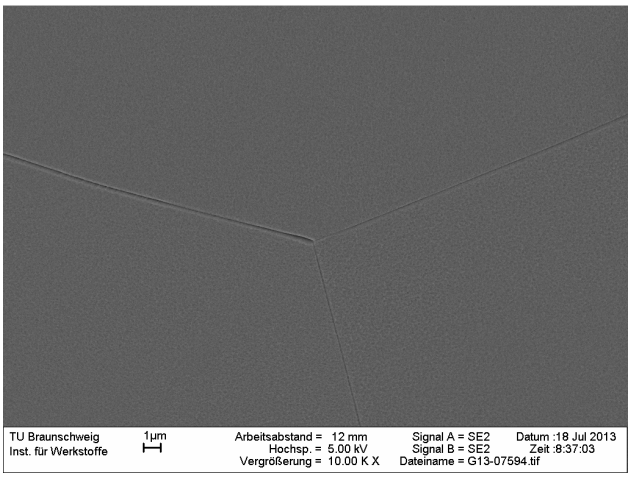

Fig. 1 Microstructure of Ti-15Mo alloy in the solution treated state, SEM

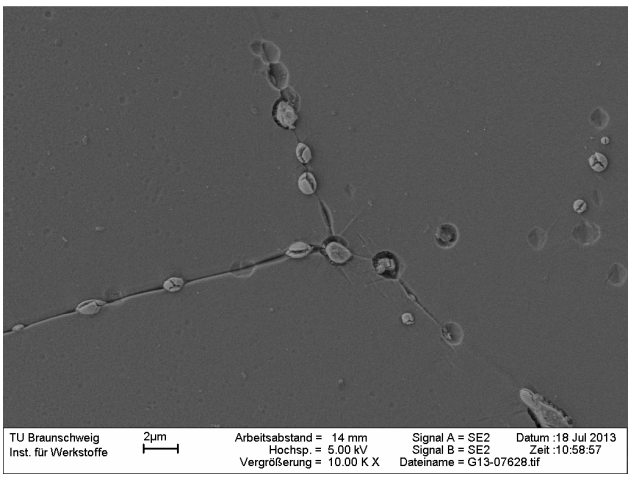

Fig. 2 Microstructure of Ti-15Mo+0.8La alloy in the solution treated state; particles are dispersed mainly on the grain boundaries, SEM

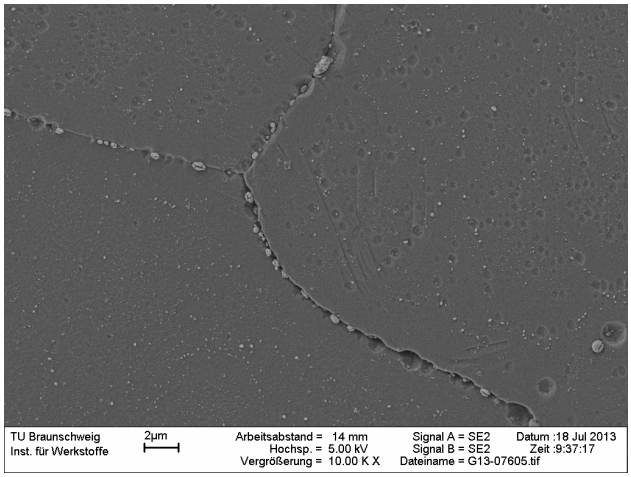

Fig. 3 Microstructure of Ti-15Mo+0.8Nd alloy in the solution treated state; particles are dispersed on grain boundaries and in the matrix, SEM

TABLE I
Comparison of the Produced Alloys in the Solution Treated State

	Ti-15Mo	+0.8La	+0.8Nd
Ø grain size	91 µm	40 µm	44 µm
max grain size	375 µm	157 µm	173 µm
particle distribution	-	grain boundary	grain boundary + matrix
max particle size	-	≈ 3 µm	≈ 2µm
Ø hardness	215 HV10	216 HV10	210 HV10

The temperatures for the compression tests were chosen with respect to the β transus temperature (T_β) of Ti-15Mo which was measured to 750°C ± 10°C. The lowest deformation temperature of 700°C was chosen to deform the alloys in the α+β field. The second temperature was 750°C (close to T_β) and the third temperature was 800°C (approx. 50 K above T_β).

The deformation below T_β led to surface cracks for all alloys. At 750°C no cracks occurred for Ti-15Mo alloy but very fine cracks were visible for both modified alloys. Finally, at 800°C just samples with lanthanum showed small cracks at the surface.

The flow stress of the modified alloys at 700°C was increased compared to the Ti-15Mo alloy. This can be explained by the finer microstructure. At 750°C and 800°C no differences in the flow stress are visible, see Table II.

TABLE II
Compression Test – Average Yield Stress of Ti-15Mo and Modified Alloys in N/mm²

Temperature	Ti-15Mo	+0.8La	+0.8Nd
700°C	184	197	204
750°C	159	152	156
800°C	133	126	129

Based on the results of the compression tests, the temperature for rotary swaging was chosen. On the one hand, to minimize grain coarsening, the temperature should be kept as low as possible. On the other hand, crack formation should

be avoided. As a compromise, the rotary swaging temperature was set to 775°C; approx. 25 K above T_β. Deformation was possible for all three alloys. No surface cracks or material failure was observed.

For the investigation of the mechanical properties in tensile tests the deformed bars were again solution treated to recover the material.

The modified alloys showed a slightly increased tensile strength compared to Ti-15Mo alloy whereas the elongation at rupture was slightly decreased but still around 30% for all alloys (see Fig. 4 and Table III). Prior investigations at Ti-6Al-4V-0.9La have shown that our laboratory-scale processing route led to inferior results compared to industrial production routes. Therefore, a better ductility can be expected if the modified alloys are industrially produced.

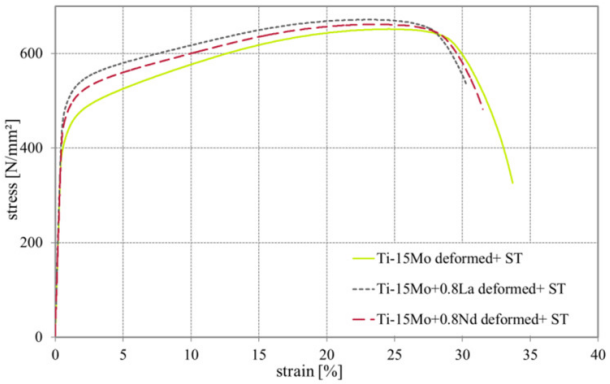

Fig. 4 Tensile Test, Ti-15Mo /+0.8La /+0.8Nd was deformed by rotary swaging at 775°C and solution treated

TABLE III
TENSILE TEST – TI-15MO AND MODIFIED ALLOYS, DEFORMED + ST

	Ti-15Mo	+0.8La	+0.8Nd
yield strength [N/mm²]	410	480	459
ultimate tensile strength [N/mm²]	652	672	662
elongation at rupture [%]	33	29	31

Extensive phase analyses were carried out at all alloys in all states. As the results were similar in all states, the ST state will be described in detail here. The Ti-15Mo alloy consisted of β-phase and nano-dispersed ω-phase which was segregated athermally. The Ti-15Mo+0.8La alloy showed β-phase and nano-dispersed ω-phase as well and three different types of lanthanum containing phases, namely, metallic cubic lanthanum and the two oxides, LaO and La_2O_3 (see Fig. 5).

Lanthanum has a strong affinity to oxygen and will oxidize immediately once exposed to air. Before ingot production, the oxide layer of the lanthanum pieces was mechanically removed before the melting but a small layer will have formed again during transport to the furnace and the evacuation procedure. In addition, lanthanum might have reacted with the oxygen dissolved in the titanium matrix which should lead to a decrease in hardness compared to the standard alloy. On the other hand, smaller grain and additional particles will increase the hardness making the detection of the mechanisms difficult.

The three lanthanum phases were still detectable in similar amounts after the heat treatments and the different deformation processes, indicating that additional particle oxidation does not occur during processing.

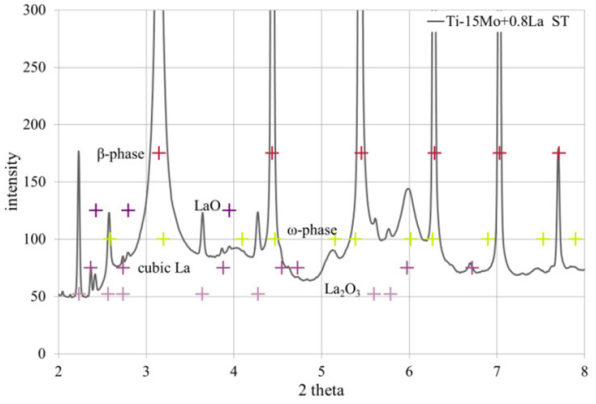

Fig. 5 Phase analyze of Ti-15Mo+0.8La in the solution treated state

The Ti-15Mo+0.8Nd alloy showed similar results. Besides β and ω, three different neodymium containing phases were observed. The related peaks were identified as pure hexagonal neodymium and the two oxides NdO_2 and Nd_2O_3.

This observation can be explained by the similar configuration of the outer electron shell of the two elements leading to similar properties.

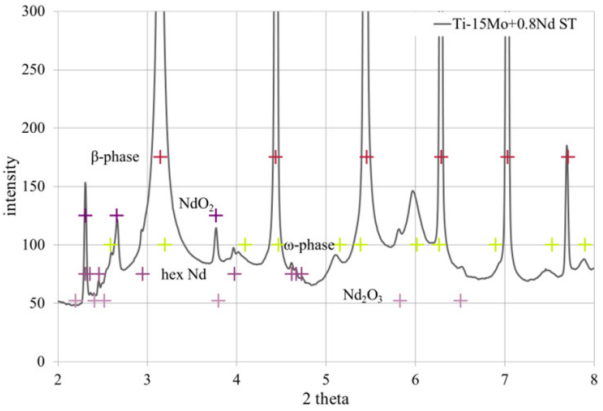

Fig. 6 Phase analyze of Ti-15Mo+0.8Nd in the solution treated state

IV. SUMMARY AND OUTLOOK

Ti-15Mo alloy was alloyed with 0.8wt.-% lanthanum and neodymium, respectively. It was observed that a static deformation below the T_β led to the formation of surface cracks. Rotary swaging at 775°C led to complete bars for all alloys. Therefore, the discovered deformation parameters can be used as starting parameters for scale-up of the alloy production. As grain coarsening has not been observed, industrial forging will be easier compared to the standard alloy as higher forging temperatures can be used.

The modified alloys showed a slightly increased tensile strength and decreased ductility in tensile test indicating that

the alloy modification did not influence the mechanical properties to a large extent.

The phase analyzes of the alloys showed β- and ω-phase in the solution treated state of all three alloys. In the modified alloys, three different rare earth metal phases were identified, namely cubic lanthanum, LaO, and La_2O_3 and hexagonal neodymium, NdO_2, and Nd_2O_3. These phases were stable during the complete process route.

As parts of the rare earth metals were precipitated as oxides they cannot act as chip breakers as their melting points are higher than 1000°C (Fig. 7). Therefore, short chip formation has not been observed so far, whereas the surface quality was already improved by the rare earth metal additions. On the other hand, the oxidic particles might stabilize the microstructure to even higher temperatures.

Fig. 7 Comparison of chip length of different titanium alloys: Ti-6Al-4V+0.9La (a), Ti-15Mo (b), and Ti-15Mo+0.8La (c)

Further research will now concentrate on modified alloys with higher amounts of the rare earth metals as deformation and tensile tests did not expose severe problems. Once the final composition has been identified, the biocompatibility has to be tested.

ACKNOWLEDGMENT

The research leading to the results presented here has been funded by the Arbeitsgemeinschaft Industrieller Forschungsvereinigungen (AiF), project number IGF 16841. Financial support is therefore greatfullly acknowledged. The research study was supported by hard X-ray experiments at PETRA III, beamline P07, HASYLAB, DESY. The authors thank U. Rütt for the scientific and technical support.

REFERENCES

[1] M. Peters, C. Leyens, *Titanium and Titanium Alloys*, Wiley-VCH, Germany, 2002.
[2] M. Geetha, A.K. Singh, R. Asokamani, A.K. Gogia, Ti based biomaterials, the ultimate choice for orthopaedic implants – A Review, Prog. Mater. Sci. 54, 2009, pp. 397-425.
[3] A.G. Robling, A.B. Castillo, C.H. Turner, Biochemical and Molecular Regulation of Bone Remodeling, Annu. Rev. Biomed. Eng. 2006, Vol. 8 (2006), pp. 455-498.
[4] A.W. Bowen, Strength enhancement in a metastable β-titanium alloy: Ti-15Mo, Journal of Mat. Sci 12, 1977, pp. 1355-1360.
[5] W. Ho, Effect of Omega Phase on Mechanical Properties of Ti-Mo Alloys for Biomedical Applications, Journal of Med. and Bio. Eng., 28(1): pp. 47-51.
[6] G. Lütjering, *Titanium*, second ed., Springer Verlag, Germany, 2007.
[7] J. Donarchie, *Titanium – A Technical Guide*, ASM International, USA, 1988.
[8] M. Bäker, Finite Element Investigation of the Flow Stress Dependence of Chip Formation, J.Mater. Proc. Technol. 167, (2005),pp. 1-13.
[9] G. Sutter, G. List, Very high speed cutting of Ti-6Al-4V titanium alloy – change in morphology and mechanism of chip formation, Int. J. of Machine Tools and Manufacture, Vol. 66, 2013, pp. 37-43.
[10] M. Cotterell, G. Byrne, Dynamics of chip formation during orthogonal cutting of titanium alloy Ti-6Al-4V, CIRP Annals – Manufacturing Techn., Vol. 57, 2008, pp. 93-96.
[11] C. Siemers, P. Jencus, M. Bäker, J. Rösler, F. Feyerabend, A new free machining Titaniumalloy containing Lanthanum, in: Proc. 11th World Conference in Ti, Kyoto, Japan (2007), pp. 709-712.
[12] C. Siemers, F. Brunke, J. Laukart, M.S. Hussain, J. Rösler, K. Saksl, B. Zahra, Rare EarthMetals in Titanium Alloys – A Systematic Study, in: Proc. COM2012, Section Rare Earth Metals 2012, Niagara Falls, Canada, 2012, pp. 281-292.
[13] J. Laukart, C. Siemers, J. Rösler, Microstructure Evolution in Ti-Al-Mo-Fe-Mn-Cr-Cu Alloyscontaining Rare-Earth Metals, in: Proc. 12th World Conference on Ti, Beijing, China (2011), pp. 459-463.
[14] J. Laukart, C. Siemers, J. Rösler, Development of a castable, free-maching titanium alloy,Mater. Sci. Forum 690, (2011), pp. 3-6.
[15] F. Brunke, E. Meyer-Kornblum, C. Siemers, Influence of Iron on the Size and Distribution of Metallic LanthanumParticles in Free-machining Titanium Alloys Ti 6Al 7Nb xFe 0.9La, Mater. Sci. Forum 765, (2013), pp. 42-46
[16] N. Schell, A. King, F. Beckmann, H.U. Ruhnau, R. Kirchhof, R. Kiehn, M. Mueller, A. Schreyer, The High Energy Materials Science Beamline (HEMS) at PETRA III, Proceedings of the 10th International Conference on Synchrotron Radiation Instrumentation, Melbourne, Australia, September 27th – October 2nd , 2009, pp. 391 – 394.
[17] A.P. Hammersley, S.O. Svensson, M. Hanfland, A.N. Fitch, D. Häusermann, Two dimensional detector software: from real detector to idealised image or two theta scan, High Pressure Research 14 (4–5), (1996), pp. 235–248.
[18] B. H. Toby, "CMPR - a powder diffraction toolkit," Journal of Applied Crystallography 38, (2005), pp. 1040-1041.
[19] C. Siemers, F. Brunke, M. Stache, J. Laukart, B. Zahra, J. Rösler, P. Rockicki, K. Saksl, Advanced Titanium Alloys containing Micrometer-Size Particles, in: Proc. 12th World Conference on Ti, Beijing, China, (2011), pp. 883-887.